IEEE Access
Multidisciplinary ⋮ Rapid Review ⋮ Open Access Journal

Received 28 February 2023, accepted 13 March 2023, date of publication 22 March 2023, date of current version 29 March 2023.

Digital Object Identifier 10.1109/ACCESS.2023.3260773

RESEARCH ARTICLE

An Adaptive Control Methodology for Spacecraft Attitude Tracking Under Model and Environmental Uncertainties

HANCHEOL CHO, (Member, IEEE)
Department of Aerospace Engineering, Embry-Riddle Aeronautical University, Daytona Beach, FL 32114, USA
e-mail: choh15@erau.edu

This work was supported by the Faculty Innovative Research in Science and Technology (FIRST) Program, Embry-Riddle Aeronautical University.

ABSTRACT This study investigates the attitude tracking problem for rigid spacecraft under model and environmental uncertainties. Two different control laws are separately developed and combined. First, based on a nominal attitude dynamic model assuming no uncertainty, the first controller is developed that exactly tracks a prespecified attitude reference trajectory with minimized control cost. The designer can generate this reference to prescribe desired performance specifications such as the maximum convergence time and overshoot. Next, an uncertain attitude dynamic system is considered, and the second controller is designed and added so that the controlled system can successfully track the predesigned reference trajectory with a user-specified tolerance even subject to uncertainty whose bounds are unknown. Compared to existing adaptive control schemes, the proposed approach possesses a very simple structure with a small number of control parameters and is not computationally intensive, making it more attractive for practical implementation. The proposed control laws generate smooth control signals and any information about the uncertainty bound is not needed in its design. Simulation results are provided to demonstrate the practical feasibility of the proposed approach, where reorientation/slew maneuvers of a large spacecraft are considered. The effects of limitations on the control torques are also investigated to show the effectiveness of the control methodology developed herein.

INDEX TERMS Attitude control, fundamental equation of constrained motion, Lyapunov stability, sliding mode control, uncertainty.

I. INTRODUCTION

Over the past few decades, the attitude tracking problem for rigid spacecraft has been the center of attention due to its broad applications to space missions such as Earth imaging, surveillance, spacecraft rendezvous and docking, on-orbit servicing, and space debris removal. However, it is still a challenging problem because the coupling between the attitude kinematics and dynamics is highly nonlinear and model and environmental uncertainties always exist [1]. To overcome these challenges, a large number of robust control methods have been explored, including proportional-integral-derivative control [2], [3], [4], backstepping control [5], [6], H_∞ control [7], [8], and adaptive fuzzy control [9], [10], [11], to list a few. Despite their efficacy, the forementioned robust control methodologies possess complicated structures with numerous control functions and parameters to be adequately chosen. Keeping a simple control structure in a closed form is critical in reliably controlling the attitude motion of a spacecraft which usually has limited computing power. In addition, in [2], [3], [4], [5], [6], [7], [8], [9], [10], and [11], no consideration was given to optimality to minimize control cost.

Sliding mode control (SMC) [12], [13], [14], [15] is favored over the other robust control methods due to its computational simplicity, fast response, easy implementation, and invariance properties. However, conventional SMC suffers from the so-called chattering effect caused by high-frequency switching control action. This drawback is partially alleviated

The associate editor coordinating the review of this manuscript and approving it for publication was Mohammad AlShabi.

by employing a boundary layer [16], which yields a loss of control accuracy. Moreover, conventional SMC requires the estimation of the upper bound on the uncertainty because the gain should be designed greater than this bound to successfully suppress uncertainty effects. The upper bound is usually estimated in a conservative manner for higher robustness, which leads to higher gain and greater chattering amplitude [17]. This is the reason the concept of *adaptive* SMC has been introduced, where the control gain is dynamically updated as the uncertainty varies with time. In [18] and [19], gain adaptation laws were devised so that the gain keeps increasing until the sliding mode is achieved. However, these laws do not allow the gain to decrease, sometimes yielding an overestimated gain and excessive chattering especially when the initial guess for the gain is selected to be too large. This drawback was remedied in [20] and [21] in which two gain update laws were proposed. The first law increases the gain until the sliding variable reaches a small domain around the origin. When the sliding variable is confined within this domain, the gain starts to decrease and keeps decreasing by the second law. Hence, the gain rate can be both positive and negative, so gain overestimation is avoided. However, the gain rate can be discontinuous at the boundary of the domain, sometimes yielding nonsmooth control signals which are not desirable. This drawback was overcome by dynamic gain adaptation where *continuous* gain adaptation laws are designed for smooth control action and applied to spacecraft formation keeping [22] and formation reconfiguration [23]. However, the controllers developed in [22] and [23] achieved only asymptotical stability and the tracking errors become bounded by a desired small domain as time goes to infinity. In practice, *finite-time* boundedness is more desirable that guarantees fast convergence of the errors and high-precision performance.

The most noticeable feature of SMC is that once the controlled system reaches the sliding surface, it is completely independent of the original dynamics and robust to the parameter variations and external disturbances [14], [15]. Nonetheless, during the reaching phase, the controlled system can be destabilized by the uncertainties and disturbances [24]. In the recent years, several methods including integral SMC [25], [26] were suggested to eliminate the reaching phase by adding a nonlinear term in the sliding surface design so that robustness is guaranteed from the beginning [17], [19], [27]. However, they did not pay attention to achieving prescribed performance in the transient and steady-state phases such as convergence time, overshoot, and control effort. It is crucial in spacecraft attitude maneuvers to achieve swift and smooth attitude change from any initial attitude while minimizing the expenditure of control effort. In brief, there has been little research in the existing literature that guarantees prespecified performance, possesses a simple structure with a small number of tuning parameters, optimally achieves finite-time boundedness of the controlled system, and generates smooth control signals in the presence of uncertainties and disturbances whose bounds are unknown.

Motivated by this discussion, in this paper a simple, adaptive smooth SMC approach is developed for precision attitude control of spacecraft in the face of model/parametric uncertainties and external disturbances whose bounds are not known *a priori*. Two different control laws are separately developed and combined. The first controller assumes a *nominal* attitude dynamics model without uncertainties or disturbances. An alternative formulation [28] in terms of the quaternion parameters will be used to describe the attitude dynamics. Unlike conventional attitude motion formulation that uses a pair of the quaternion and the angular velocity, this formulation employs a pair of the quaternion and its time derivative. Then, a nominal reference trajectory for each quaternion parameter to track will be designed to achieve a desired, prescribed performance in terms of maximum convergence time and overshoot, and an exact real-time controller will be obtained in a closed form with the use of the fundamental equation of constrained motion [29]. This controller considers the tracking requirements as equality constraints and provides the exact optimal control law that minimizes the control cost at each instant of time. For the second controller, based on the notion of SMC, an adaptive compensating control law will be designed for on-orbit attitude tracking for the uncertain system to mitigate any uncertainty effects not considered in the first step. In [30], the robust attitude tracking problem was tackled using the formulation and approach given in [28] and [29], but it was assumed that the upper bound on the uncertainty is *a priori* known. On the contrary, the proposed controller will automatically update its gain and *a priori* knowledge of the uncertainty bound is not required. Also, the generated control signals will be smooth and the controlled quaternion parameters will successfully track the nominal trajectory designed in the first step. By defining a tracking error as the difference between the actual quaternion trajectory and the nominal trajectory, the sliding variable always starts with zero and therefore the reaching phase is removed. This greatly simplifies the controller design and significantly enhances the stability and robustness of the controlled system throughout the controlled motion. Although the tracking error is not exactly regulated to be zero, it will be bounded by a small tolerance in finite time and the user can always impose an allowed maximum error bound on tracking performance. It will also be shown that compared to existing adaptive control schemes, the proposed control laws possess a very simple structure with a small number of control parameters. The main contributions of this study can be summarized as follows:

- Unlike the robust control methodologies shown in [5], [6], [7], [8], [22], [23], and [30], in this paper *finite-time smooth* adaptive control laws are proposed for precision attitude control. The tracking errors are bounded by a user-specified small ball in finite time from any initial condition under model uncertainties and disturbances whose bounds are *unknown*.
- The size of the error ball can be directly prespecified by the user.

- *Desired transient performance* such as overshoot and convergence rate is guaranteed to achieve swift and smooth attitude change from any initial attitude.
- Compared to the existing adaptive control strategies [5], [6], [7], [8], [9], [10], [11], [12], [13], the proposed controller possesses a *simple structure* with known functions and a minimum number of adaptive tuning parameters, which is of vital importance in attitude control of a real-world spacecraft with limited computing power. The effect of each control parameter on the control performance is also provided. It is shown that the proposed control law can lead to adaptive proportional-derivative (PD) control or proportional-integral-derivative (PID) control as a special case.
- Different from the works [2], [3], [4], [5], [6], [7], [8], [9], [10], [11], [12], [13], the control methodology in this paper considers *optimality* in its design. Without uncertainties or disturbances, the proposed control laws will be optimal and minimize the control cost at each instant of time. When uncertainties or disturbances are present, the second control law will precisely eliminate their effects and the controlled system will behave as the nominal system for which the first control law enables the exact tracking of the nominal trajectory with the minimized control cost.

This paper is organized as follows. In Section II the description of constrained dynamic systems is reviewed, which serves as a prelude to Section III. In Section III the equation of attitude motion will be introduced in terms of quaternion parameters and their derivatives, based on which the subsequent control laws will be developed. Section IV deals with the design of the nominal reference trajectory for the quaternions to track by considering prescribed performance. The first controller will also be designed using the fundamental equation of constrained motion assuming a nominal system with no uncertainties. In Section V, the second compensating controller is developed to track the nominal trajectory designed in Section IV, assuming parameter uncertainties and environmental disturbances. In addition, the gain adaptation law will be proposed and the finite-time boundedness of the controlled system will be proven via Lyapunov's direct method. A brief explanation about the effect of control parameters on the performance will also be provided. Section VI provides numerical simulations to demonstrate the ease and accuracy of the combined control laws developed in Sections IV and V, and the performance is compared with the one obtained using an existing method. The effect of saturation on the control torques is also simulated and discussed to show the effectiveness of the proposed methodology. Finally, Section VII concludes this paper.

II. CONSTRAINED DYNAMIC SYSTEMS

This section reviews an approach to describe the motion of constrained dynamical systems. Any attitude requirements on the spacecraft will be viewed as constraints on the dynamic system, and an explicit equation of motion will be introduced to satisfy these requirements. The equation of motion will be used to derive a new form of the attitude dynamics and to obtain exact control torques for a nominal system without uncertainties or disturbances.

Without any constraints, the equation of motion of a dynamic system is usually given, using the Lagrange equation, by

$$\mathbf{M}(\boldsymbol{q}, t)\,\ddot{\boldsymbol{q}} = \boldsymbol{Q}(\boldsymbol{q}, \dot{\boldsymbol{q}}, t), \tag{1}$$

or

$$\ddot{\boldsymbol{q}}(t) = \mathbf{M}^{-1}(\boldsymbol{q}, t)\,\boldsymbol{Q}(\boldsymbol{q}, \dot{\boldsymbol{q}}, t) \triangleq \boldsymbol{a}(t), \tag{2}$$

where $\boldsymbol{q}(t) = \left[\, q_1(t)\ q_2(t)\ \cdots\ q_n(t) \,\right]^T \in \mathbb{R}^n$ is the generalized coordinate vector, t is time, $\mathbf{M}(\boldsymbol{q}, t) \in \mathbb{R}^{n\times n}$ is the positive-definite mass matrix, $\boldsymbol{Q}(\boldsymbol{q}, \dot{\boldsymbol{q}}, t) \in \mathbb{R}^n$ is a 'given' force vector, and $\boldsymbol{a}(t) \in \mathbb{R}^n$ is the unconstrained acceleration vector. The superscript "T" denotes the transpose of a vector or a matrix.

The system given by (1) or (2) is now subjected to p constraints of the form

$$\varphi_j(\boldsymbol{q}, \dot{\boldsymbol{q}}, t) = 0, j = 1, 2, \cdots, p. \tag{3}$$

If we differentiate (3) once (for nonholonomic constraints) or twice (for holonomic constraints) with respect to time, the following constraint equation is obtained:

$$\mathbf{A}(\boldsymbol{q}, \dot{\boldsymbol{q}}, t)\,\ddot{\boldsymbol{q}}(t) = \boldsymbol{b}(\boldsymbol{q}, \dot{\boldsymbol{q}}, t), \tag{4}$$

where $\mathbf{A}(\boldsymbol{q}, \dot{\boldsymbol{q}}, t) \in \mathbb{R}^{p\times n}$ and $\boldsymbol{b}(\boldsymbol{q}, \dot{\boldsymbol{q}}, t) \in \mathbb{R}^p$. From here on, the arguments of the various quantities will be suppressed for brevity unless required for clarity. The presence of the constraints in (4) forces the equation of motion to have the form of

$$\mathbf{M}\ddot{q} = \boldsymbol{Q} + \boldsymbol{Q}_c, \tag{5}$$

where $\boldsymbol{Q}_c \in \mathbb{R}^n$ is the vector of constraint forces by which the constraint equation (4) is satisfied. It is known that the constraint forces can always be written as [29]

$$\boldsymbol{Q}_c = -\mathbf{A}^T\boldsymbol{\lambda}, \tag{6}$$

where $\mathbf{A}$ is the matrix shown in (4) and $\boldsymbol{\lambda} \in \mathbb{R}^p$ is the vector of Lagrange multipliers. Then, (4) and (5) can be expressed in a compact form as

$$\begin{bmatrix} \mathbf{M} & \mathbf{A}^T \\ \mathbf{A} & \mathbf{0} \end{bmatrix} \begin{bmatrix} \ddot{\boldsymbol{q}} \\ \boldsymbol{\lambda} \end{bmatrix} = \begin{bmatrix} \boldsymbol{Q} \\ \boldsymbol{b} \end{bmatrix}. \tag{7}$$

The coefficient matrix in (7) is symmetric and invertible if the matrix $\mathbf{A}$ has a full rank so that

$$\begin{bmatrix} \ddot{\boldsymbol{q}} \\ \boldsymbol{\lambda} \end{bmatrix} = \begin{bmatrix} \mathbf{M} & \mathbf{A}^T \\ \mathbf{A} & \mathbf{0} \end{bmatrix}^{-1} \begin{bmatrix} \boldsymbol{Q} \\ \boldsymbol{b} \end{bmatrix} = \begin{bmatrix} \mathbf{S}_{qq} & \mathbf{S}_{q\lambda} \\ \mathbf{S}_{\lambda q} & \mathbf{S}_{\lambda\lambda} \end{bmatrix} \begin{bmatrix} \boldsymbol{Q} \\ \boldsymbol{b} \end{bmatrix}, \tag{8}$$

where the elements of the inverse of the 2 by 2 block matrix is given by [31]

$$\begin{aligned}\mathbf{S}_{qq} &= \left(\mathbf{I}-\mathbf{M}^{-1}\mathbf{A}^T\left(\mathbf{A}\mathbf{M}^{-1}\mathbf{A}^T\right)^{-1}\mathbf{A}\right)\mathbf{M}^{-1},\\ \mathbf{S}_{q\lambda} &= \mathbf{S}_{\lambda q}^T = \mathbf{M}^{-1}\mathbf{A}^T\left(\mathbf{A}\mathbf{M}^{-1}\mathbf{A}^T\right)^{-1},\\ \mathbf{S}_{\lambda\lambda} &= -\left(\mathbf{A}\mathbf{M}^{-1}\mathbf{A}^T\right)^{-1}.\end{aligned} \tag{9}$$

Hence, the vectors of the accelerations and Lagrange multipliers can be explicitly computed as

$$\begin{bmatrix}\ddot{\boldsymbol{q}}\\ \boldsymbol{\lambda}\end{bmatrix} = \begin{bmatrix}\boldsymbol{a}+\mathbf{M}^{-1}\mathbf{A}^T\left(\mathbf{A}\mathbf{M}^{-1}\mathbf{A}^T\right)^{-1}(\boldsymbol{b}-\mathbf{A}\boldsymbol{a})\\ -\left(\mathbf{A}\mathbf{M}^{-1}\mathbf{A}^T\right)^{-1}(\boldsymbol{b}-\mathbf{A}\boldsymbol{a})\end{bmatrix}, \tag{10}$$

where $\boldsymbol{a}=\mathbf{M}^{-1}\boldsymbol{Q}$ is used. From (10), the constraint force is explicitly obtained as

$$\boldsymbol{Q}_c = \mathbf{A}^T\left(\mathbf{A}\mathbf{M}^{-1}\mathbf{A}^T\right)^{-1}(\boldsymbol{b}-\mathbf{A}\boldsymbol{a}). \tag{11}$$

If the matrix $\mathbf{A}$ is rank-deficient, i.e., all the constraints are not independent of each other, the coefficient matrix in (7) is not invertible, and more than one solution $\left[\ddot{\boldsymbol{q}}^T\ \boldsymbol{\lambda}^T\right]^T$ may exist. The solution can be uniquely determined if it is chosen to minimize the cost $J=(\ddot{\boldsymbol{q}}-\boldsymbol{a})^T\mathbf{W}(\ddot{\boldsymbol{q}}-\boldsymbol{a})$ at each instant of time, where $\mathbf{W}>\mathbf{0}$ is a weight matrix. It is shown in [32] that the optimal solution $\ddot{\boldsymbol{q}}$ minimizing the cost J is uniquely given by

$$\ddot{\boldsymbol{q}} = \boldsymbol{a}+\mathbf{M}^{-1}\mathbf{W}^{-1}\mathbf{M}\mathbf{A}^T\left(\mathbf{A}\mathbf{M}^{-1}\mathbf{W}^{-1}\mathbf{M}\mathbf{A}^T\right)^{+}(\boldsymbol{b}-\mathbf{A}\boldsymbol{a}), \tag{12}$$

where the superscript "+" denotes the Moore-Penrose generalized inverse. If the weight matrix is chosen as $\mathbf{W}=\mathbf{M}$ to match Gauss' principle [33], the equation of motion for a constrained dynamic system is simply given by

$$\ddot{\boldsymbol{q}} = \boldsymbol{a}+\mathbf{M}^{-1}\mathbf{A}^T\left(\mathbf{A}\mathbf{M}^{-1}\mathbf{A}^T\right)^{+}(\boldsymbol{b}-\mathbf{A}\boldsymbol{a}). \tag{13}$$

Equation (13) is called the *fundamental equation of constrained motion* (FECM) and it is always valid whether the matrix $\mathbf{A}$ has a full rank or not. Accordingly, the constraint force is obtained as

$$\boldsymbol{Q}_c = \mathbf{A}^T\left(\mathbf{A}\mathbf{M}^{-1}\mathbf{A}^T\right)^{+}(\boldsymbol{b}-\mathbf{A}\boldsymbol{a}). \tag{14}$$

Note that (10) and (11) are special cases of (13) and (14). In this paper, (13) and (14) will be used to compute the exact control torques to achieve pointing requirements with no uncertainties. Attitude requirements will be viewed as constraints and so the terms *requirements* and *constraints* will be interchangeably used. Accordingly, the constraint force/torque explicitly given in (14) will be used to obtain the control force/torque for the nominal system (with no uncertainties), in order to satisfy the constraints of the form of (4). It should be noted that the control force/torque given by (14) is the *optimal* solution that minimizes the control cost $J=(\ddot{\boldsymbol{q}}-\boldsymbol{a})^T\mathbf{M}(\ddot{\boldsymbol{q}}-\boldsymbol{a})=\boldsymbol{Q}_c^T\mathbf{M}^{-1}\boldsymbol{Q}_c$ *at each instant of time*.

III. SPACECRAFT ATTITUDE DYNAMICS

Spacecraft attitude dynamics can be described in terms of quaternion parameters to avoid the singularity issue. In [28], a new method to derive the attitude dynamics with the use of the FECM was proposed, which is employed in this paper. Assuming no uncertainties, the attitude equation of motion is given by [28]

$$\ddot{\boldsymbol{q}} = -\frac{1}{2}\mathbf{E}_1^T\mathbf{J}^{-1}\left[\tilde{\boldsymbol{\omega}}\right]\mathbf{J}\boldsymbol{\omega}-N(\dot{\boldsymbol{q}})\,\boldsymbol{q}+\mathbf{M}_q^{-1}\boldsymbol{\Gamma}_c, \tag{15}$$

where $\boldsymbol{q}=[q_0,q_1,q_2,q_3]^T=\left[q_0,\tilde{\boldsymbol{q}}^T\right]^T=\left[\cos(\theta/2),\hat{\boldsymbol{e}}^T\sin(\theta/2)\right]^T$ is the quaternion vector of the spacecraft, $\hat{\boldsymbol{e}}\in\mathbb{R}^3$ is a unit vector defined relative to an inertial coordinate frame, θ is the rotation angle about the unit vector $\hat{\boldsymbol{e}}$, $\boldsymbol{\omega}=\left[\omega_x,\omega_y,\omega_z\right]^T$ is the angular velocity vector of the spacecraft along its body-fixed coordinate frame, $\left[\tilde{\boldsymbol{\omega}}\right]$ is the skew-symmetric matrix multiplication, $\mathbf{J}=\mathrm{diag}\left\{J_x,J_y,J_z\right\}>\mathbf{0}$ is the nominal moment of inertia matrix of the spacecraft, $N(\dot{\boldsymbol{q}})=\dot{q}_0^2+\dot{q}_1^2+\dot{q}_2^2+\dot{q}_3^2$, and

$$\mathbf{E}_1 = \begin{bmatrix}-q_1 & q_0 & q_3 & -q_2\\ -q_2 & -q_3 & q_0 & q_1\\ -q_3 & q_2 & -q_1 & q_0\end{bmatrix}. \tag{16}$$

Furthermore, $\mathbf{M}_q=4\mathbf{E}^T\hat{\mathbf{J}}\boldsymbol{E}>0$ is a 4 by 4 nominal mass matrix where $\hat{\mathbf{J}}=\mathrm{diag}\{J_0,\mathbf{J}\}=\mathrm{diag}\left\{J_0,J_x,J_y,J_z\right\}>0$ is a 4 by 4 augmented inertia matrix with an arbitrary positive number J_0, and

$$\mathbf{E}=\begin{bmatrix}\boldsymbol{q}^T\\ \mathbf{E}_1\end{bmatrix}=\begin{bmatrix}q_0 & q_1 & q_2 & q_3\\ -q_1 & q_0 & q_3 & -q_2\\ -q_2 & -q_3 & q_0 & q_1\\ -q_3 & q_2 & -q_1 & q_0\end{bmatrix}, \tag{17}$$

which is orthogonal, i.e., $\mathbf{E}^{-1}=\mathbf{E}^T$. The vector $\boldsymbol{\Gamma}_c$ in (15) is the 4 by 1 generalized quaternion torque and is related to the 3 by 1 physically applied torque about the body axis, $\boldsymbol{Q}_c=\left[Q_{c,x},Q_{c,y},Q_{c,z}\right]^T$, through the relation

$$\boldsymbol{Q}_c = \frac{1}{2}\mathbf{E}_1\boldsymbol{\Gamma}_c. \tag{18}$$

It is noted that the time derivative of the quaternion vector $\dot{\boldsymbol{q}}$ is related with the angular velocity as

$$\{\boldsymbol{\omega}\} = 2\mathbf{E}\dot{q}, \tag{19}$$

where $\{\boldsymbol{\omega}\}=\left[0,\boldsymbol{\omega}^T\right]^T=\left[0,\omega_x,\omega_y,\omega_z\right]^T$ is the 4 by 1 augmented angular velocity vector. Unlike conventional formulation using the 7-order pair $(\boldsymbol{q},\boldsymbol{\omega})$, this paper will utilize the 8-order pair $(\boldsymbol{q},\dot{\boldsymbol{q}})$ that will ease the sliding surface design and subsequent controller design. One can easily switch from one to the other through the use of (19).

In the next section, by ignoring any uncertainties or disturbances, an exact control torque $\boldsymbol{Q}_c(t)$ will be obtained for the *nominal* system for which the equation of motion is fully and exactly known.

IV. EXACT CONTROL FOR NOMINAL SYSTEM WITH NO UNCERTAINTIES

In this paper, two different control methods will be explored that force the spacecraft to follow the desired attitude trajectory by effectively suppressing the effect of uncertainties or disturbances. The first controller is developed in this section in which a nominal system is considered assuming no uncertainties and an exact control torque is explicitly obtained using the FECM. The attitude tracking requirements are viewed as constraints on the nominal system that can be expressed in the form of (4).

The equation of motion for the nominal system is given by (15) and we rewrite it as.

$$\ddot{\boldsymbol{q}} = \boldsymbol{a} + \mathbf{M}_q^{-1}\boldsymbol{\Gamma}_c, \tag{20}$$

where $\boldsymbol{a} = -(1/2)\,\mathbf{E}_1^T\mathbf{J}^{-1}\left[\tilde{\boldsymbol{\omega}}\right]\mathbf{J}\boldsymbol{\omega} - N(\dot{\boldsymbol{q}})\,\boldsymbol{q}$. Now, the controlled state vector $\boldsymbol{q}(t)$ is required to follow a desired quaternion vector $\boldsymbol{q}_d(t)$ to satisfy attitude requirements by the application of the control torque $\boldsymbol{Q}_c(t)$, or equivalently, $\boldsymbol{\Gamma}_c(t)$. Let us assume that the desired quaternion vector is given by

$$\boldsymbol{q}_d(t) = \left[\, q_{d,0}(t)\ q_{d,1}(t)\ q_{d,2}(t)\ q_{d,3}(t) \,\right]^T, \tag{21}$$

where $q_{d,i}(t)$, $i = 0, 1, 2, 3$ is a desired quaternion function. Now the constraint equation is written as

$$\begin{bmatrix} q_0(t) - q_{d,0}(t) \\ q_1(t) - q_{d,1}(t) \\ q_2(t) - q_{d,2}(t) \\ q_3(t) - q_{d,3}(t) \end{bmatrix} = \begin{bmatrix} 0 \\ 0 \\ 0 \\ 0 \end{bmatrix}. \tag{22}$$

The constraint equation (22) must be satisfied at all times along with the quaternion norm constraint given by $q_0^2 + q_1^2 + q_2^2 + q_3^2 = 1$ or

$$q_0\ddot{q}_0 + q_1\ddot{q}_1 + q_2\ddot{q}_2 + q_3\ddot{q}_3 = -\dot{q}_0^2 - \dot{q}_1^2 - \dot{q}_2^2 - \dot{q}_3^2. \tag{23}$$

In a general situation attitude control is initiated from a different quaternion vector, yielding initial errors in (22). Hence, let us consider the following modified constraint equation obtained by Baumgarte's stabilization technique [34]:

$$\ddot{\boldsymbol{\Phi}}(t) + \alpha\dot{\boldsymbol{\Phi}}(t) + \beta\boldsymbol{\Phi}(t) = \mathbf{0}, \tag{24}$$

where $\boldsymbol{\Phi}(t) = \left[\, q_1 - q_{d,1}\ q_2 - q_{d,2}\ q_3 - q_{d,3} \,\right]^T$ is a 3 by 1 vector, and α and β are positive constants that determine the behavior of the second-order damped system. For example, the designer can select the values for α and β to prescribe the maximum convergence time of the controlled system with no overshoot. Then, it is guaranteed that as time progresses, the constraint vector $\boldsymbol{\Phi}(t)$ will asymptotically decay to zero from any initial conditions with a prespecified convergence time and with no overshoot. The remaining quaternion element $q_0(t)$ will be determined to satisfy the constraint (23). The combined constraint equations (23) and (24) can now be written in a matrix form as

$$\underbrace{\begin{bmatrix} q_0 & q_1 & q_2 & q_3 \\ 0 & 1 & 0 & 0 \\ 0 & 0 & 1 & 0 \\ 0 & 0 & 0 & 1 \end{bmatrix}}_{\mathbf{A}} \underbrace{\begin{bmatrix} \ddot{q}_0 \\ \ddot{q}_1 \\ \ddot{q}_2 \\ \ddot{q}_3 \end{bmatrix}}_{\ddot{\boldsymbol{q}}} = \underbrace{\begin{bmatrix} -\dot{q}_0^2 - \dot{q}_1^2 - \dot{q}_2^2 - \dot{q}_3^2 \\ \ddot{q}_{d,1} - \alpha\left(\dot{q}_1 - \dot{q}_{d,1}\right) - \beta\left(q_1 - q_{d,1}\right) \\ \ddot{q}_{d,2} - \alpha\left(\dot{q}_2 - \dot{q}_{d,2}\right) - \beta\left(q_2 - q_{d,2}\right) \\ \ddot{q}_{d,3} - \alpha\left(\dot{q}_3 - \dot{q}_{d,3}\right) - \beta\left(q_3 - q_{d,3}\right) \end{bmatrix}}_{\boldsymbol{b}}, \tag{25}$$

which is of the form of (4). Finally, the 4 by 1 generalized control torque is obtained as

$$\boldsymbol{\Gamma}_c = \mathbf{A}^T\left(\mathbf{A}\mathbf{M}_q^{-1}\mathbf{A}^T\right)^+(\boldsymbol{b} - \mathbf{A}\boldsymbol{a}), \tag{26}$$

where $\mathbf{M}_q = 4\mathbf{E}^T\hat{\mathbf{J}}\boldsymbol{E}$, $\boldsymbol{a} = -(1/2)\,\mathbf{E}_1^T\mathbf{J}^{-1}\left[\tilde{\boldsymbol{\omega}}\right]\mathbf{J}\boldsymbol{\omega} - N(\dot{\boldsymbol{q}})\,\boldsymbol{q}$, and $\mathbf{A}$ and $\boldsymbol{b}$ are given in (25). Note that the matrix $\mathbf{A}$ becomes singular when $q_0 = 0$ and so the regular inverse $\left(\mathbf{A}\mathbf{M}_q^{-1}\mathbf{A}^T\right)^{-1}$ cannot be used. The 3 by 1 physically applied torque $\boldsymbol{Q}_c$ is explicitly obtained as

$$\boldsymbol{Q}_c = \frac{1}{2}\mathbf{E}_1\boldsymbol{\Gamma}_c = \frac{1}{2}\mathbf{E}_1\mathbf{A}^T\left(\mathbf{A}\mathbf{M}_q^{-1}\mathbf{A}^T\right)^+(\boldsymbol{b} - \mathbf{A}\boldsymbol{a}). \tag{27}$$

Since (27) is obtained by assuming no uncertainties, an additional control torque should be added to compensate for their effects, which will be developed in the next section.

Remark 1: When there is no uncertainty in the system, the control torque $\boldsymbol{Q}_c$ given in (27) will force the quaternion parameters to exactly follow the constrained trajectory given in (25) while minimizing the control cost $J = \boldsymbol{Q}_c^T\mathbf{M}_q^{-1}\boldsymbol{Q}_c$ at each instant of time.

V. ROBUST ADAPTIVE CONTROL FOR ACTUAL, UNCERTAIN SYSTEM

The nominal system assumes a perfect model for attitude dynamics with no uncertainties/disturbances. In real-life applications, this assumption does not hold, and the nominal control torque (27) will no longer make the requirement $\boldsymbol{q}(t) = \boldsymbol{q}_d(t)$ satisfied. Hence, to successfully follow the desired quaternion trajectory in the presence of uncertainties/disturbances, we need to add an additional control torque vector $\boldsymbol{Q}_r(t) = (1/2)\,\mathbf{E}_1\boldsymbol{\Gamma}_r(t)$ so that the equation of motion of the actual, uncertain system becomes

$$\ddot{\boldsymbol{q}} = -\frac{1}{2}\mathbf{E}_1^T\tilde{\mathbf{J}}^{-1}\left[\tilde{\boldsymbol{\omega}}\right]\tilde{\mathbf{J}}\boldsymbol{\omega} - N(\dot{\boldsymbol{q}})\,\boldsymbol{q} + \tilde{\mathbf{M}}_q^{-1}\left(\boldsymbol{\Gamma}_c + \boldsymbol{\Gamma}_r + \boldsymbol{\delta}\right), \tag{28}$$

where $\tilde{\mathbf{J}}$ and $\tilde{\mathbf{M}}_q$ are the unknown, actual moment of inertia and mass matrices, respectively, the term $\boldsymbol{\delta}(t)$ contains all the external disturbances or perturbations, and the solution $\boldsymbol{q}(t)$ will then successfully follow $\boldsymbol{q}_d(t)$ with a proper design of the compensating controller $\boldsymbol{\Gamma}_r$. For low-Earth satellites or spacecraft, the vector $\boldsymbol{\delta}(t)$ is mainly caused by solar array deployment, aerodynamic torque, magnetic torque, solar radiation

torque, and gravity-gradient torque, and it is known that these disturbance values are bounded [35], [36].

The aim of this section is to design a robust controller $\boldsymbol{\Gamma}_r$ such that the controlled quaternion vector $\boldsymbol{q}(t)$ successfully follows the *nominal* trajectory $\boldsymbol{q}_n(t)$ generated as the solution to (20) satisfying the constraint equation (25) even in the presence of uncertainties or disturbances; the *nominal* quaternion vector $\boldsymbol{q}_n(t)$ should not be confused with $\boldsymbol{q}_d(t)$, the *desired* quaternion vector, given by (21), satisfying (22) where $\alpha = \beta = 0$. Any nonzero initial errors will yield $\boldsymbol{q}_n(t) \neq \boldsymbol{q}_d(t)$ at the initial time. However, if we define a 4 by 1 error vector as

$$\boldsymbol{e}(t) \triangleq \boldsymbol{q}(t) - \boldsymbol{q}_n(t), \tag{29}$$

the initial error vector $\boldsymbol{e}(0)$ is zero because the nominal trajectory always starts from the current state. The error definition (29) will greatly ease the design of a sliding surface and remove the reaching phase so that robustness is guaranteed from the beginning.

The compensating controller $\boldsymbol{\Gamma}_r(t)$ or $\boldsymbol{Q}_r(t)$ will be designed by generalizing the concept of sliding mode control (SMC). Unlike conventional SMC that suffers from chattering caused by discontinuous control signals [14], [15], the proposed method will produce continuous control action. More specifically, the designed controller will nudge the sliding variables so that their norm always lies within a prespecified small 'ball' around the nominal trajectory $\boldsymbol{q}_n(t)$. Also, exact information about the uncertainty bound is not necessary because the control law is adjusted in an adaptive manner. For the sake of brevity, let us consider the linear sliding surface (another nonlinear sliding surface can be used depending on the application):

$$\boldsymbol{s}(t) \triangleq \dot{\boldsymbol{e}}(t) + \lambda \boldsymbol{e}(t), \tag{30}$$

where $\boldsymbol{s}(t) = \left[\, s_0(t)\ s_1(t)\ s_2(t)\ s_3(t) \,\right]^T$ and $\boldsymbol{e}(t) = \left[\, e_0(t)\ e_1(t)\ e_2(t)\ e_3(t) \,\right]^T$ is the error vector defined in (29). Also, λ is a positive constant to be selected by the user that determines the control accuracy. In general, a larger λ yields a smaller tracking error, as shall be shown later. It should be noted that $\boldsymbol{s}(0) = \boldsymbol{0}$, meaning that the sliding mode starts from the initial time and the system's trajectory always starts on the sliding surface. The time derivative of (30) yields

$$\begin{aligned}\dot{\boldsymbol{s}} &= \ddot{\boldsymbol{e}} + \lambda \dot{\boldsymbol{e}} \\ &= \left(\ddot{\boldsymbol{q}} - \ddot{\boldsymbol{q}}_n\right) + \lambda\left(\dot{\boldsymbol{q}} - \dot{\boldsymbol{q}}_n\right) \\ &= -\frac{1}{2}\mathbf{E}_1^T \tilde{\mathbf{J}}^{-1}\left[\tilde{\boldsymbol{\omega}}\right]\tilde{\mathbf{J}}\boldsymbol{\omega} - N(\dot{\boldsymbol{q}})\,\boldsymbol{q} + \tilde{\mathbf{M}}_q^{-1}\left(\boldsymbol{\Gamma}_c + \boldsymbol{\Gamma}_r + \boldsymbol{\delta}\right) \\ &\quad - \ddot{\boldsymbol{q}}_n + \lambda\left(\dot{\boldsymbol{q}} - \dot{\boldsymbol{q}}_n\right).\end{aligned} \tag{31}$$

If the actual mass matrix is decomposed into $\tilde{\mathbf{M}}_q = \mathbf{M}_q + \delta\mathbf{M}$ where $\mathbf{M}_q$ is the nominal (known) mass matrix and $\delta\mathbf{M}$ is the unknown part, then the following is satisfied [37]:

$$\begin{aligned}\tilde{\mathbf{M}}_q^{-1} &= \mathbf{M}_q^{-1} - \mathbf{M}_q^{-1}\left(I + \delta\mathbf{M}\cdot\mathbf{M}_q^{-1}\right)^{-1}\delta\mathbf{M}\cdot\mathbf{M}_q^{-1} \\ &= \mathbf{M}_q^{-1} + \boldsymbol{\Delta}_M,\end{aligned} \tag{32}$$

where $\boldsymbol{\Delta}_M$ is unknown. Then, (31) becomes

$$\dot{\boldsymbol{s}} = \boldsymbol{\Delta} + \mathbf{M}_q^{-1}\boldsymbol{\Gamma}_r, \tag{33}$$

where

$$\begin{aligned}\boldsymbol{\Delta} = &-\frac{1}{2}\mathbf{E}_1^T\tilde{\mathbf{J}}^{-1}\left[\tilde{\boldsymbol{\omega}}\right]\tilde{\mathbf{J}}\boldsymbol{\omega} - N(\dot{\boldsymbol{q}})\,\boldsymbol{q} - \ddot{\boldsymbol{q}}_n + \lambda\left(\dot{\boldsymbol{q}} - \dot{\boldsymbol{q}}_n\right) \\ &+ \mathbf{M}_q^{-1}\left(\boldsymbol{\Gamma}_c + \boldsymbol{\delta}\right) + \boldsymbol{\Delta}_M\left(\boldsymbol{\Gamma}_c + \boldsymbol{\Gamma}_r + \boldsymbol{\delta}\right)\end{aligned} \tag{34}$$

is uncertain. In this paper, it is assumed that during the control time interval (or maneuver time) $t \in [0, t_f]$ the uncertain 4 by 1 vector $\boldsymbol{\Delta}(t)$ is bounded by

$$\|\boldsymbol{\Delta}(t)\| < \bar{\Delta}, \tag{35}$$

where $\|\cdot\|$ is the infinity norm of a vector and $\bar{\Delta}$ is an *unknown* positive constant. This assumption is valid because the disturbance term $\boldsymbol{\delta}(t)$ is bounded, the control time interval is finite, the magnitude of any control torques is physically limited, and the designed control law will guarantee the finite-time boundedness of the closed-loop system, as shall be shown shortly.

Let us consider the following compensating control law:

$$\boldsymbol{\Gamma}_r(t) = -|K(t)|\,\mathbf{M}_q\left(\frac{\boldsymbol{s}(t)}{\varepsilon}\right)^{\rho}, \tag{36}$$

where

$$\left(\frac{\boldsymbol{s}(t)}{\varepsilon}\right)^{\rho} = \left[\, \left(\tfrac{s_0(t)}{\varepsilon}\right)^{\rho}\ \left(\tfrac{s_1(t)}{\varepsilon}\right)^{\rho}\ \left(\tfrac{s_2(t)}{\varepsilon}\right)^{\rho}\ \left(\tfrac{s_3(t)}{\varepsilon}\right)^{\rho} \,\right]^T, \tag{37}$$

ρ is a positive odd integer ($\rho = 1, 3, 5, \cdots$) and ε is a user-specified (small) positive constant. It is noted that mass matrix $\mathbf{M}_q$ is the nominal one, which is known. Although the form of the control law (36) is similar to the one proposed in [30], it was assumed in [30] that the upper bound on the uncertainty is *a priori* known and so a constant gain was used. On the contrary, in this paper the control gain $K(t)$ is updated by the following adaptation rule:

$$\dot{K}(t) = \begin{cases} 0, \text{ if } \|\boldsymbol{s}(t)\| \leq \gamma\varepsilon \\ \mu\,\|\boldsymbol{s}(t)\|\left(\left\|\dfrac{\boldsymbol{s}(t)}{\varepsilon}\right\| - \kappa\right), \text{ otherwise} \end{cases} \tag{38}$$

where $0 < \gamma, \kappa < 1$ are constants and μ is a positive constant that regulates the rate of the gain change. The initial condition is chosen to satisfy $0 < K(0) \leq \bar{\Gamma}\gamma^{-\rho}$, where $\bar{\Gamma}$ is the control acceleration limit that shall be given in (39). It is noted that when the infinity norm of the sliding variable vector $\|\boldsymbol{s}(t)\|$ is greater than the threshold ε, the controller increases the gain, i.e., $\dot{K}(t) > 0$.

Remark 2: The first controller given in (27) is automatically determined once we select $\mathbf{A}$ *and* $\boldsymbol{b}$ *to satisfy a prescribed performance. In designing the second controller*

given in (36), six parameters $(\lambda, \varepsilon, \rho, \gamma, \mu, \kappa)$ *are to be selected. The influence of each parameter on the performance is as follows:*

1) *The two parameters* λ, ε *in (30) and (36) determine control accuracy so that the sliding variable and the tracking error in the steady-state are bounded by* $\|\boldsymbol{s}\| \leq \varepsilon$ and $\|\boldsymbol{e}\| \leq \varepsilon/\lambda$, *respectively, as shall be proven in Theorem 2. If* ε *is selected too small, numerical instability may occur in discrete-time implementation unless the sampling period is sufficiently small. This is because the sliding variable needs to be sufficiently frequently controlled to be smaller than* ε *under uncertainties/disturbances that may be fast varying.*
2) *The parameter* ρ *in (36) describes the sensitivity of the variation in the sliding variable on the control input. Because of the term* $(\boldsymbol{s}/\varepsilon)^{\rho}$, *a larger* ρ *yields a greater control torque* $\boldsymbol{\Gamma}_r$ *when* $\|\boldsymbol{s}\| > \varepsilon$, *but a smaller torque when* $\|\boldsymbol{s}\| < \varepsilon$ *(compared to a smaller* ρ*). For example, when* $\|\boldsymbol{s}\| > \varepsilon$ *holds, a larger* ρ *enables faster convergence of the sliding variable and the error to the region* $\|\boldsymbol{s}\| < \varepsilon$, *but the resulting steady-state error would be larger than the case with a smaller* ρ. *In most cases, it is sufficient to choose* $\rho = 1$ *or 3.*
3) *The parameter* γ *in (38) determines when to stop the gain update. When* $\|\boldsymbol{s}\| \leq \gamma\varepsilon$, *the gain is not updated any more and maintains the value* $K(t_i)$, *where* t_i *is the instant at which the condition* $\|\boldsymbol{s}(t)\| \leq \gamma\varepsilon$ *starts to hold. A larger* γ *yields a static gain more often.*
4) *The parameter* μ *in (38) regulates the rate of change in the gain. A larger* μ *enables a rapid gain change but an excessive* μ *may yield instability of the controlled system. The control law with too small* μ *cannot catch up with the variation of the uncertainty and so robustness may be lost. A rule of thumb for* μ *is to set it between 0.1 and 1.0.*
5) *The parameter* κ *in (38) determines when to increase or decrease the gain. It is obvious from (38) that when* $\|\boldsymbol{s}/\varepsilon\| > \kappa$, K *increases, otherwise, it decreases. A smaller* κ *makes the gain increase more easily. A sufficiently small* κ *will continuously increase the gain until the condition* $\|\boldsymbol{s}\| \leq \gamma\varepsilon$ *is met and the gain gets saturated at a high value, yielding a smaller error compared to when a larger* κ *is selected.*

Remark 3: If the linear sliding surface (30) is used and $\rho = 1$ *is selected in (36), then the controller (36) becomes a simple PD controller with the adaptive gain so that*

$$\boldsymbol{\Gamma}_r(t) = -\frac{|K(t)|}{\varepsilon}\mathbf{M}_q\left[\dot{\boldsymbol{e}}(t) + \lambda\boldsymbol{e}(t)\right], \tag{39}$$

where $K(t)$ *is updated by (38). If an integral term is added to the sliding surface, the controller becomes an adaptive PID controller. In this sense, the proposed gain adaptation rule can provide a simple method for PD/PID gain tuning.*

Now we propose two theorems. The first theorem states that the gain has an upper bound if the magnitude of the control torque is limited (because any physical actuators cannot generate infinite torques). The second theorem guarantees the finite-time boundedness of the uncertain attitude dynamic system controlled by the robust adaptive control algorithm proposed in (36) and (38).

Theorem 1: Assume that the magnitude of the control acceleration is limited such that

$$\left\|\mathbf{M}_q^{-1}(t)\,\boldsymbol{\Gamma}_r(t)\right\| \leq \bar{\Gamma}, \tag{40}$$

where $\bar{\Gamma}$ *is a known positive constant. Then, the magnitude of the gain always has an upper bound such that*

$$|K(t)| \leq \bar{\Gamma}\gamma^{-\rho}. \tag{41}$$

Proof: From (36), we have

$$\left\|\mathbf{M}_q^{-1}\boldsymbol{\Gamma}_r(t)\right\| = |K(t)|\left\|\frac{\boldsymbol{s}(t)}{\varepsilon}\right\|^{\rho}. \tag{42}$$

First, consider the case when $\gamma\varepsilon < \|\boldsymbol{s}(t)\|$ is satisfied. Then, $\gamma^{\rho} < \|\boldsymbol{s}(t)/\varepsilon\|^{\rho}$ holds, and so

$$\gamma^{\rho}|K| \leq |K|\left\|\frac{\boldsymbol{s}}{\varepsilon}\right\|^{\rho}. \tag{43}$$

From (40), (42), and (43), $\gamma^{\rho}|K| \leq \bar{\Gamma}$ is derived and so (41) is proven.

Next, let us consider the case when $\|\boldsymbol{s}(t)\| \leq \gamma\varepsilon$. In this case, $\dot{K} = 0$ and the gain K maintains the value $K(t_i)$, where t_i is the instant when the condition $\|\boldsymbol{s}(t)\| \leq \gamma\varepsilon$ starts to hold. Since $|K(t)| \leq \bar{\Gamma}\gamma^{-\rho}$ is always satisfied when $\|\boldsymbol{s}(t)\| > \gamma\varepsilon$, $|K(t_i)|$ should also be less than or equal to $\bar{\Gamma}\gamma^{-\rho}$. Hence, for both cases (41) is always satisfied and Theorem 1 is proven. ■

Theorem 2: Assume that the control acceleration has an upper limit $\bar{\Gamma}$ *as given in (40). Then, for the uncertain attitude dynamic system (28), the controller designed as in (36) with the gain adaptation law (38) will cause the sliding variable vector defined in (30) to be bounded by* $\|\boldsymbol{s}(t)\| \leq \varepsilon$ *in finite time from any state. Also, the tracking error will be confined in the region* $\|\boldsymbol{e}(t)\| \leq \varepsilon/\lambda$.

Proof: Let us define the following Lyapunov function:

$$V(t) = \frac{1}{2}\boldsymbol{s}(t)^T\boldsymbol{s}(t) + \frac{1}{2\tilde{\mu}}(K(t) - \Upsilon)^2, \tag{44}$$

where $0 < \tilde{\mu} \leq \mu(1-\kappa)/2$ is a constant and Υ is a constant satisfying $\Upsilon > \max\left(\bar{\Gamma}\gamma^{-\rho}, 4\bar{\Delta}\right)$. First, consider the case when $\|\boldsymbol{s}(t)\| > \varepsilon$ holds. If we can show that $\dot{V} < -\Lambda V^{1/2}, \Lambda > 0$ being constant for $\|\boldsymbol{s}(t)\| > \varepsilon$, then finite-time convergence to the domain $\|\boldsymbol{s}(t)\| \leq \varepsilon$ is guaranteed, where the convergence time is estimated as $t_F \leq 2V^{1/2}(t_0)/\Lambda$ with t_0 being the instant at which $\|\boldsymbol{s}(t)\| > \varepsilon$ starts to hold [38], [39].

From Theorem 1, $|K(t)| \leq \bar{\Gamma}\gamma^{-\rho} < \Upsilon$ holds and the differentiation of (44) with respect to time yields

$$\begin{aligned}\dot{V} &= \boldsymbol{s}^T\dot{\boldsymbol{s}} + \frac{1}{\tilde{\mu}}(K-\Upsilon)\dot{K} \\ &= \boldsymbol{s}^T\left(\boldsymbol{\Delta} + \mathbf{M}_q^{-1}\boldsymbol{\Gamma}_r\right) + \frac{1}{\tilde{\mu}}(K-\Upsilon)\dot{K} \\ &= \boldsymbol{s}^T\left(\boldsymbol{\Delta} - |K|\left(\frac{\boldsymbol{s}}{\varepsilon}\right)^{\rho}\right) + \frac{1}{\tilde{\mu}}(K-\Upsilon)\dot{K} \\ &< 4\|\boldsymbol{s}\|\bar{\Delta} - |K|\boldsymbol{s}^T\left(\frac{\boldsymbol{s}}{\varepsilon}\right)^{\rho} + \frac{1}{\tilde{\mu}}(K-\Upsilon)\dot{K}, \end{aligned} \tag{45}$$

where the last inequality is derived because

$$\boldsymbol{s}^T\boldsymbol{\Delta} < \|s_0\|\bar{\Delta} + \|s_1\|\bar{\Delta} + \|s_2\|\bar{\Delta} + \|s_3\|\bar{\Delta} \leq 4\|\boldsymbol{s}\|\bar{\Delta}. \tag{46}$$

Since $\boldsymbol{s}^T(\boldsymbol{s}/\varepsilon)^{\rho} \geq \|\boldsymbol{s}\|\|\boldsymbol{s}/\varepsilon\|^{\rho} > \|\boldsymbol{s}\|$ and $K(t) < \Upsilon$, we have

$$\begin{aligned}\dot{V} &< 4\|\boldsymbol{s}\|\bar{\Delta} - |K|\|\boldsymbol{s}\| + \frac{1}{\tilde{\mu}}(K-\Upsilon)\dot{K} \\ &= \|\boldsymbol{s}\|\left(4\bar{\Delta} - |K|\right) + \frac{1}{\tilde{\mu}}(K-\Upsilon)\dot{K} + \|\boldsymbol{s}\|\Upsilon - \|\boldsymbol{s}\|\Upsilon \\ &= \|\boldsymbol{s}\|\left(4\bar{\Delta} - \Upsilon\right) + \frac{1}{\tilde{\mu}}(K-\Upsilon)\dot{K} - \|\boldsymbol{s}\|(|K| - \Upsilon) \\ &\leq -\|\boldsymbol{s}\|\Lambda_s - (\Upsilon - K)\left(-\|\boldsymbol{s}\| + \frac{1}{\tilde{\mu}}\dot{K}\right), \end{aligned} \tag{47}$$

where $\Lambda_s\Upsilon - 4\bar{\Delta} > 0$ and $\Upsilon > |K| \geq K$ are used. One can rewrite the last line of (47) as

$$\begin{aligned}\dot{V} &< -\Lambda_s\|\boldsymbol{s}\| - (\Upsilon-K)\left(-\|\boldsymbol{s}\| + \frac{1}{\tilde{\mu}}\dot{K}\right) \\ &\quad + \varepsilon(\Upsilon-K) - \varepsilon(\Upsilon-K) \\ &= -\Lambda_s\|\boldsymbol{s}\| - \underbrace{(\Upsilon-K)\left(-\|\boldsymbol{s}\| + \frac{1}{\tilde{\mu}}\dot{K} - \varepsilon\right)}_{\xi} - \varepsilon(\Upsilon-K) \\ &= -\Lambda_s\sqrt{2}\cdot\frac{\|\boldsymbol{s}\|}{\sqrt{2}} - \varepsilon\sqrt{2\tilde{\mu}}\cdot\frac{\Upsilon-K}{\sqrt{2\tilde{\mu}}} - \xi \\ &\leq -\sqrt{2}\min\left\{\Lambda_s, \varepsilon\sqrt{\tilde{\mu}}\right\}\left(\frac{\|\boldsymbol{s}\|}{\sqrt{2}} + \frac{\Upsilon-K}{\sqrt{2\tilde{\mu}}}\right) - \xi \\ &\leq -\Lambda\cdot V^{1/2} - \xi, \end{aligned} \tag{48}$$

where $\Lambda = \sqrt{2}\min\left\{\Lambda_s, \varepsilon\sqrt{\tilde{\mu}}\right\} > 0$. If ξ is made positive or equal to zero by properly selecting the parameter $\tilde{\mu}$, then we guarantee $\dot{V} < -\Lambda\cdot V^{1/2} - \xi \leq -\Lambda\cdot V^{1/2}$ and the finite-time convergence to the region $\|\boldsymbol{s}(t)\| \leq \varepsilon$ is proven.

Since $\Upsilon - K > 0$, the condition $\xi \geq 0$ yields $\dot{K}/\tilde{\mu} - \|\boldsymbol{s}\| - \varepsilon \geq 0$ or

$$\tilde{\mu} \leq \frac{\dot{K}}{\|\boldsymbol{s}\| + \varepsilon} = \underbrace{\mu\frac{\|\boldsymbol{s}\|\left(\left\|\frac{\boldsymbol{s}}{\varepsilon}\right\| - \kappa\right)}{\|\boldsymbol{s}\| + \varepsilon}}_{\Phi}, \tag{49}$$

where (38) was used. Since we consider the region where $\|\boldsymbol{s}(t)\| > \varepsilon$ holds, we have

$$\Phi > \mu\frac{\|\boldsymbol{s}\|(1-\kappa)}{\|\boldsymbol{s}\| + \varepsilon} > \frac{\mu(1-\kappa)}{2}. \tag{50}$$

Since $0 < \tilde{\mu} \leq \mu(1-\kappa)/2$, (49) is satisfied and so we obtain $\dot{V} < -\Lambda\cdot V^{1/2} - \xi \leq -\Lambda\cdot V^{1/2}$. In brief, if $\|\boldsymbol{s}\|$ is outside the compact set $\Omega_\varepsilon = \left\{\boldsymbol{s} \in \mathbb{R}^4 : \|\boldsymbol{s}\| \leq \varepsilon\right\}$, then $\dot{V} < -\Lambda\cdot V^{1/2}$ and a decreasing value of V will eventually drive $\|\boldsymbol{s}\|$ into the set Ω_ε in finite time $t_F \leq 2V^{1/2}(t_0)/\Lambda$. Hence, the set Ω_ε is attractive and $\|\boldsymbol{s}\|$ is bounded thanks to Lyapunov stability theory [38], [39].

Next, when $\|\boldsymbol{s}(t)\| \leq \varepsilon$ holds, the sign of $\dot{V}$ is indefinite and it is possible for $\|\boldsymbol{s}(t)\|$ to become greater than ε. However, as soon as $\|\boldsymbol{s}(t)\| > \varepsilon$ holds, $\dot{V} < -\Lambda\cdot V^{1/2}$ is satisfied and $\|\boldsymbol{s}(t)\|$ will again be bounded by ε in finite time, as previously shown.

Hence, by applying the control law (36) with the gain adaptation rule (38), $\|\boldsymbol{s}(t)\|$ will be bounded by $\|\boldsymbol{s}(t)\| \leq \varepsilon$ in finite time from any state. Finally, while the condition $\|\boldsymbol{s}(t)\| \leq \varepsilon$ is satisfied, it can be readily shown [39] that the error is bounded by $\|\boldsymbol{e}(t)\| \leq \varepsilon/\lambda$, where $\boldsymbol{s}(t)$ and $\boldsymbol{e}(t)$ are related to each other by (30). This completes the proof. ■

In summary, the controller design procedure is given as follows:

Step 1. Assuming no uncertainty and disturbance, create a desired quaternion vector $\boldsymbol{q}_d(t)$ so that the prescribed performance is satisfied. Find the corresponding matrix $\mathbf{A}$ and vector $\boldsymbol{b}$ in the form of (25).

Step 2. Design the first controller $\boldsymbol{Q}_c$ for the nominal system using (27). This controller minimizes the control cost $J = \boldsymbol{Q}_c^T\mathbf{M}_q^{-1}\boldsymbol{Q}_c$ when there is no uncertainty.

Step 3. Now, model uncertainty and external disturbance are considered. Select appropriate parameters λ, ε, ρ, γ, μ, and κ by referring to the discussion in Remark 2. Choose the initial gain so that $0 < K(0) \leq \bar{\Gamma}\gamma^{-\rho}$.

Step 4. Design the second controller $\boldsymbol{Q}_r = (1/2)\mathbf{E}_1\boldsymbol{\Gamma}_r$, where $\boldsymbol{\Gamma}_r$ is given in (36) with the gain adaption law (38). This controller eliminates the effects of uncertainties and disturbances so that the controlled system behaves as the nominal system described by (20) with no uncertainty and disturbance.

VI. SIMULATION RESULTS

To verify their robustness and accuracy, the two control methods proposed in the previous sections are applied to a rest-to-rest slew maneuver. The simulations are carried out in the MATLAB/Simulink environment and a fixed time-step ode4 Runge-Kutta integrator with the sampling period of 0.01 s is used.

Consider a Hubble Space Telescope-like spacecraft whose mass is 13,000 kg. Its nominal moment of inertia is given by $\mathbf{J} = \text{diag}\left[35997\ 86852\ 93913\right]\left(\text{kg}\cdot\text{m}^2\right)$ and a 10% uncertainty is considered so that its actual moment of inertia is given by $\hat{\mathbf{J}} = \mathbf{J} + 0.1\mathbf{J} = \text{diag}\left[39596.795537.2103304.3\right]\left(\text{kg}\cdot\text{m}^2\right)$ which is unknown to us. It is assumed that the external disturbances are mainly induced by the solar array along the y-axis [35] so that $\hat{\boldsymbol{\delta}}(t) = [00.2\sin(2\pi(0.12)t) + 0.2\sin(2\pi(0.66)t)0]^T$ $(\text{N}\cdot\text{m})$ and a 4 by 1 vector $\boldsymbol{\delta}(t)$ that is shown in (28) is obtained as $\boldsymbol{\delta}(t) = 2\mathbf{E}_1^T\hat{\boldsymbol{\delta}}(t)$. The initial values for the quaternion and

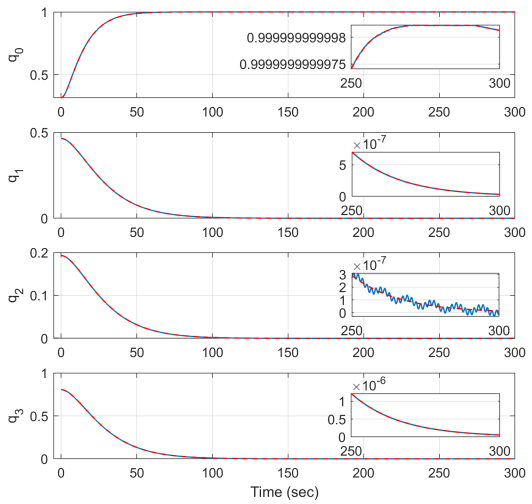

FIGURE 1. Time history of quaternions of the controlled system (Red: reference, Blue: controlled).

angular velocity are chosen similar to the ones used in [40]:

$$\boldsymbol{q}(0) = \left[0.3153\ 0.4646\ 0.1928\ 0.8047\right]^T,$$
$$\boldsymbol{\omega}(0) = \left[0\ 0\ 0\right]^T \text{(rad/s)}. \tag{51}$$

Then, the initial value for the quaternion derivative is found by (19) as $\dot{\boldsymbol{q}}(0) = (1/2)\,\mathbf{E}^T(0)\{\boldsymbol{\omega}(0)\} = \left[0\ 0\ 0\ 0\right]^T$. The desired quaternion and angular velocity are selected as

$$\boldsymbol{q}_d(t) = \left[1\ 0\ 0\ 0\right]^T,$$
$$\boldsymbol{\omega}_d(t) = \left[0\ 0\ 0\right]^T \text{(rad/s)}, \tag{52}$$

and so the desired maneuver angle is 2.5 rad. For the nominal trajectory $\boldsymbol{q}_n(t)$ to be tracked, $\alpha = 0.13$ and $\beta = \alpha^2/4 = 0.004225$ are carefully chosen to satisfy the desired output performance: 1. critical damping is achieved with no overshoot; and 2. the quaternion parameters q_1, q_2, and q_3 should converge to less than 0.01 within 100 sec. Although a rest-to-rest slew maneuver is considered in this example, it equivalently becomes a time-varying attitude tracking problem in which the reference command is given by (25). As for the robust controller, the following parameters are chosen:

$$\lambda = 5, \varepsilon = 0.01, \rho = 1,$$
$$\gamma = 0.001, \mu = 1, \kappa = 0.5, K(0) = 0.1. \tag{53}$$

First, we assume an unconstrained case where there is no limit on control torques applied or the maximum torque that the actuator can apply is sufficiently large. Figure 1 shows the time history of the quaternion parameters. The red dashed line denotes the nominal reference trajectory and the blue solid line represents the controlled one. It is seen that the spacecraft quaternions converge to less than 0.01 within 100 sec as required and successfully approach the desired values specified by (52). Figure 2 plots the time history of the corresponding Euler angles (roll-pitch-yaw), all of which converge to zero. In Figure 3, the time history of the tracking

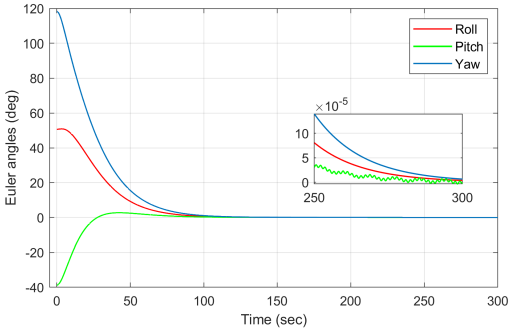

FIGURE 2. Time history of Euler angles (roll-pitch-yaw).

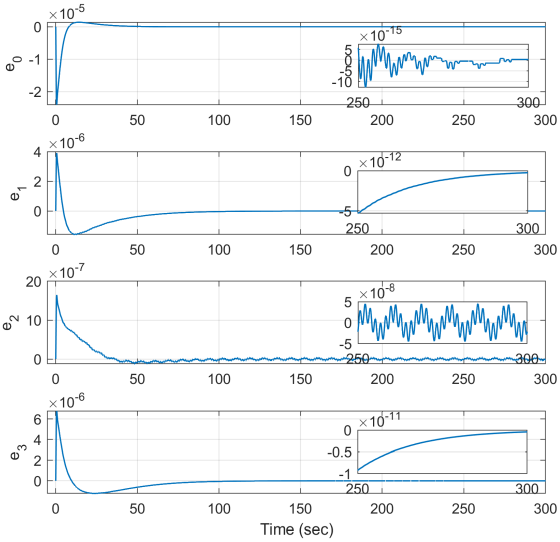

FIGURE 3. Quaternion tracking errors between the controlled and nominal quaternion trajectories.

error (29) is depicted that indicates the discrepancy between the controlled and nominal trajectories. After 250 seconds, the upper bound on the quaternion errors are of the order of 10^{-8} although external disturbances caused by the solar array and 10% inertia uncertainty are induced. This error bound is much smaller than the one expected by Theorem 2, i.e., $\varepsilon/\lambda = 0.002$. The time history of the angular velocity in each axis is shown in Figure 4. The steady-state error is found of the order of 10^{-7}. Figure 5 shows the nominal control torques ($\boldsymbol{Q}_c(t)$, red line), the robust control torques ($\boldsymbol{Q}_r(t)$, green line), and the total control torques ($\boldsymbol{Q}_c(t) + \boldsymbol{Q}_r(t)$, blue line) for each axis. It is seen that the magnitude of the nominal control torques are relatively larger than the one of the robust control torques that are needed to suppress the effects of the uncertainty. Figure 6 plots the time history of the sliding variables, showing that its infinity norm is well bounded by ε. The time history of the adaptive gain $K(t)$ is also provided in Figure 7. While the condition $\|\boldsymbol{s}\| \leq \varepsilon$ is satisfied, $K(t)$ keeps decreasing as indicated by Theorem 1 and maintains constant once $\|\boldsymbol{s}\|$ becomes less than $\gamma\varepsilon = 10^{-5}$. The control performances shown in Figures 1-7 indicate that the proposed control law can successfully perform large angle slew maneuvers.

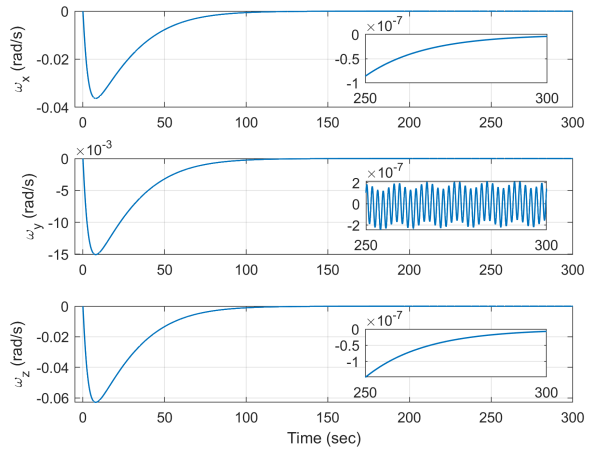

FIGURE 4. Time history of the angular velocity of the controlled system.

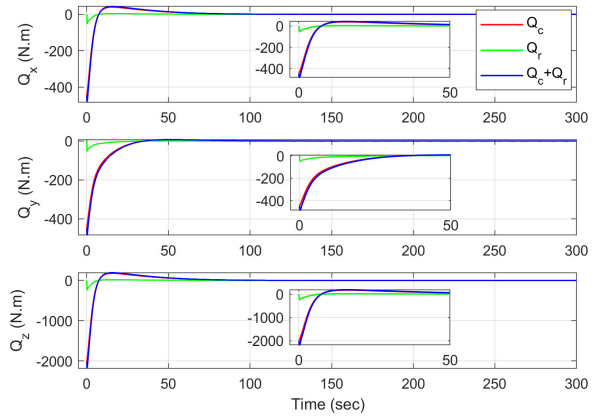

FIGURE 5. Time history of nominal control torques (Q_c), robust control torques (Q_r), and total control torques ($Q_c + Q_r$).

TABLE 1. Comparison of controllers.

Controller	Peak control torque	Torque at 300 sec	Angular velocity at 300 sec	Quaternion norm at 300 sec
	$\max\{\|\boldsymbol{Q}_c+\boldsymbol{Q}_r\|_2\}$ $(\mathrm{N}\cdot\mathrm{m})$	$\|\boldsymbol{Q}_c+\boldsymbol{Q}_r\|_2$ $(\mathrm{N}\cdot\mathrm{m})$	$\|\boldsymbol{\omega}\|_2$ (rad/sec)	$\left\|[q_1,q_2,q_3]^T\right\|_2$
Controller in [5]	49668.00	0.11	2.77e-7	2.34e-6
Proposed controller	2291.74	0.059	1.44e-7	6.61e-8

The simulation results obtained using the proposed method are compared with the ones of [5] under the same condition. The controller proposed in [5] utilized the backstepping control method with a nonlinear tracking function and the gains were selected based on a redesigned Lyapunov function. However, the upper bound on the uncertainties should be known in advance to guarantee the stability of the controlled system. The control parameters are reselected to yield the same performance: no overshoot and the maximum convergence time of 100 sec.

The simulation results of [5] are provided in Figures 8-10. Compared with the existing method proposed in [5], the

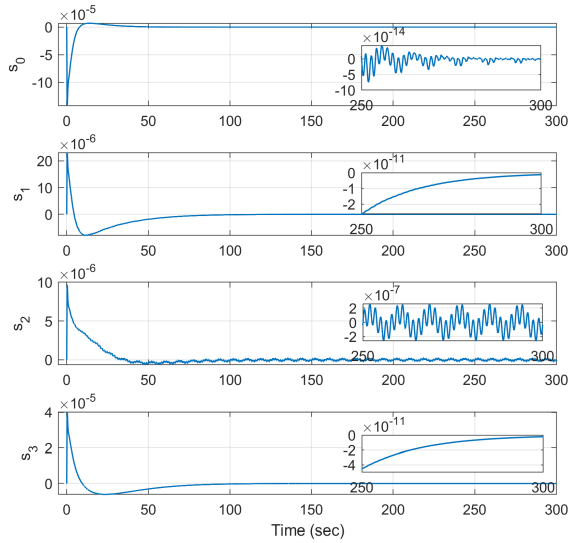

FIGURE 6. Time history of sliding variables.

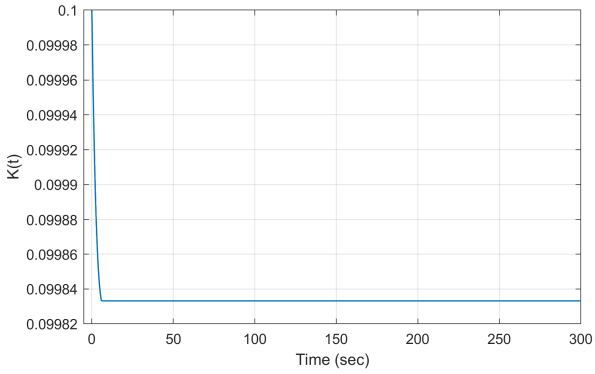

FIGURE 7. Time history of adaptive gain.

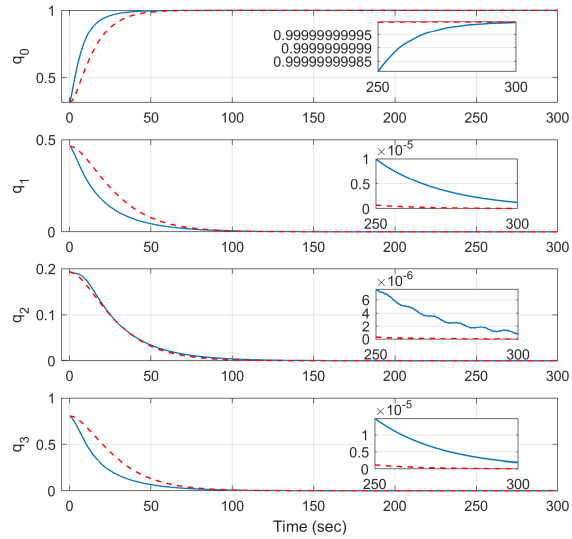

FIGURE 8. Time history of quaternions when the controller proposed in [5] is used (Blue) and when the controller in this paper is used (Red).

robust control methodology developed in this paper provides better performance. The quaternion parameters converge to the desired values in similar settling times (but with a little larger rise times), but the steady-state errors are smaller and

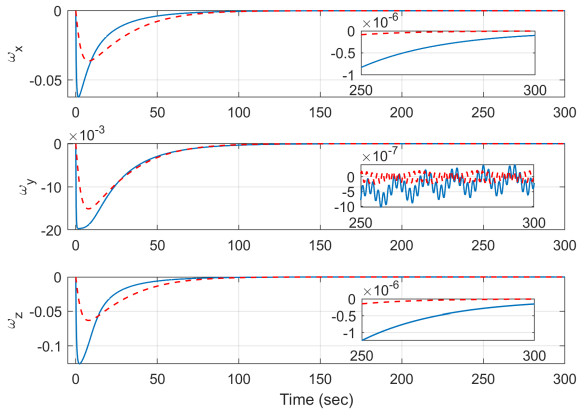

FIGURE 9. Time history of angular velocity when the controller in [5] is used (Blue) and when the controller in this paper is used (Red).

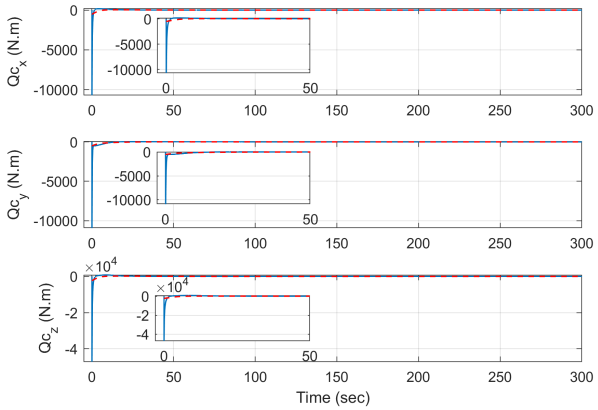

FIGURE 10. Time history of control torques when the controller in [5] is used (Blue) and the controller in this paper is used (Red).

the required control torques are also much smaller. Table 1 lists the peak control torque, as well as the control torque, angular velocity norm, and quaternion norm at 300 sec for both controllers. The peak control torque generated by the proposed control method is 2291.74 (N·m) while the existing controller requires 49668.00 (N·m). The values of $\|\boldsymbol{Q}_c + \boldsymbol{Q}_r\|_2$, $\|\boldsymbol{\omega}\|_2$, and $\left\|\begin{bmatrix} q_1 & q_2 & q_3 \end{bmatrix}^T\right\|_2$ at 300 sec also reveal smaller steady-state errors and control cost when using the proposed controller.

Finally, let us investigate the performance of the robust control laws proposed in the current paper in the presence of limitations imposed on the magnitude of the control torques. It is assumed that the magnitude of the total control torque $\boldsymbol{Q} = \boldsymbol{Q}_c + \boldsymbol{Q}_r$ is now saturated at 1600 $\mathrm{N \cdot m}$ in each axis. From Figure 5 it is expected that the control torques would be saturated at the beginning in the z-direction. Figure 11 shows the time history of the nominal control torques ($\boldsymbol{Q}_c$), the robust control torques ($\boldsymbol{Q}_r$), and the total control torques ($\boldsymbol{Q}_c + \boldsymbol{Q}_r$) for each axis. As expected, the control torque in the z-direction gets saturated for the first 5 seconds. Although each of the control torques $\boldsymbol{Q}_c$ and $\boldsymbol{Q}_r$ may exceed the limit (1600 $\mathrm{N \cdot m}$), their sum - the actual control command applied to the actuator - is always bounded by this limit. In Figure 12 the time history of the quaternion parameters is provided.

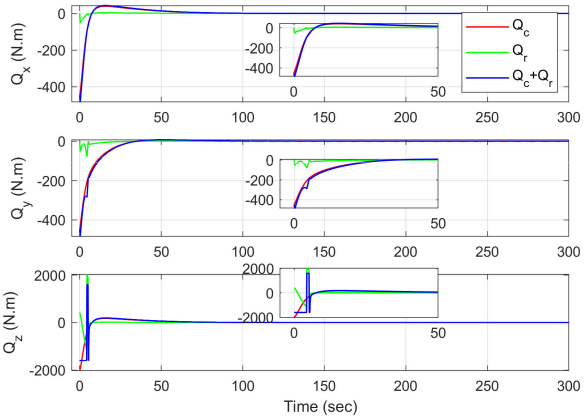

FIGURE 11. Time history of nominal control torques (Q_c), robust control torques (Q_r), and total control torques ($Q_c + Q_r$) when control torques are saturated at 1600 N•m.

TABLE 2. Comparison of controllers.

Controller	Peak control torque $\max\{\|\boldsymbol{Q}_c + \boldsymbol{Q}_r\|_2\}$ $(\mathrm{N \cdot m})$	Torque at 300 sec $\|\boldsymbol{Q}_c + \boldsymbol{Q}_r\|_2$ $(\mathrm{N \cdot m})$	Angular velocity at 300 sec $\|\boldsymbol{\omega}\|_2$ (rad/sec)	Quaternion norm at 300 sec $\left\|[q_1, q_2, q_3]^T\right\|_2$
Controller in [5]	2771.18	0.11	2.85e-7	2.59e-6
Proposed controller	1740.61	0.034	9.72e-8	6.61e-8

Even in the presence of control torque saturation, the quaternions are successfully controlled to follow the nominal reference trajectory. Figure 13 depicts the time history of the corresponding Euler angles (roll-pitch-yaw). They converge to zero as desired. In Figure 14, the time history of the tracking errors is plotted. Compared with Figure 3 where the control input is not constrained, the maximum errors are larger due to the saturation, but the steady-state errors are a little smaller. The same behavior can be seen in Figures 15 and 16 where the time history of the angular velocity and the sliding variable is presented, respectively. One can observe that the angular velocity and the sliding variable have larger values in the reaching phase than the ones in Figures 4 and 6 due to the control input saturation, but the steady-state errors are a little smaller. The control gain plotted in Figure 17 explains the reason. In Figure 7 the gain keeps decreasing because the condition $\|\boldsymbol{s}/\varepsilon\| - \kappa < 0$ is always satisfied throughout the simulation and gets stabilized to 0.09983 once the condition $\|\boldsymbol{s}\| \leq \gamma\varepsilon$ is met (see (38)). On the contrary, in Figure 17 the gain keeps increasing because in the reaching phase $\|\boldsymbol{s}/\varepsilon\| - \kappa > 0$ and so $\dot{K} > 0$ holds. Once the condition $\|\boldsymbol{s}\| \leq \gamma\varepsilon$ is satisfied, the gain gets stabilized at 0.1509. According to (36), a larger $|K|$ is equivalent to a smaller ε, and so the higher gain in the constrained case causes the smaller steady-state errors.

The performance obtained using the proposed controller in the presence of control torque saturation is compared with

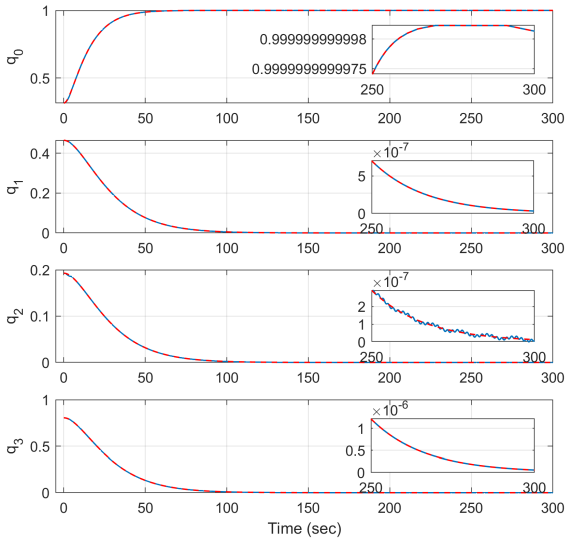

FIGURE 12. Time history of quaternion parameters when control torques are saturated at 1600 N•m (Red: reference, Blue: controlled).

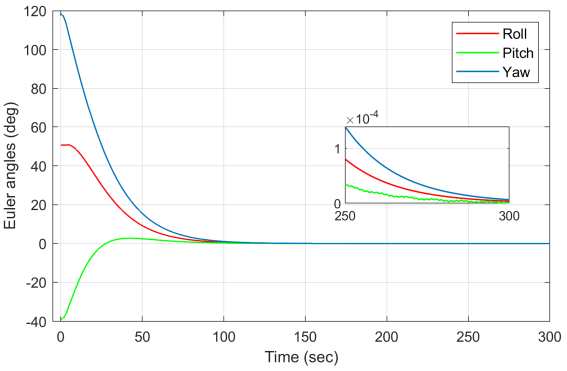

FIGURE 13. Time history of Euler angles (roll-pitch-yaw) when control torques are saturated at 1600 N•m.

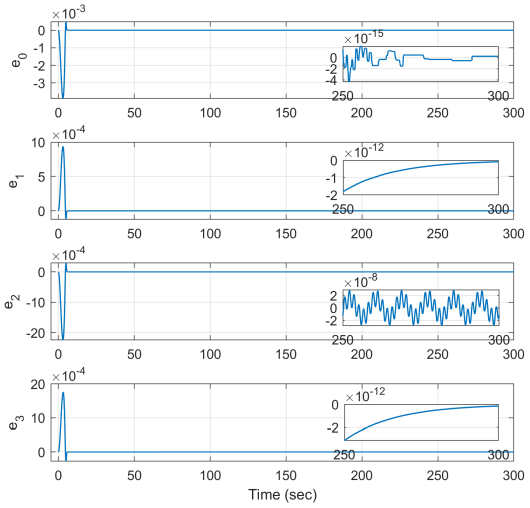

FIGURE 14. Quaternion tracking errors between the controlled and nominal trajectories when control torques are saturated at 1600 N•m.

one obtained using the method shown in [5]. The simulation results are presented in Figures 18-20. Again, the robust control methodology proposed in this paper yields better

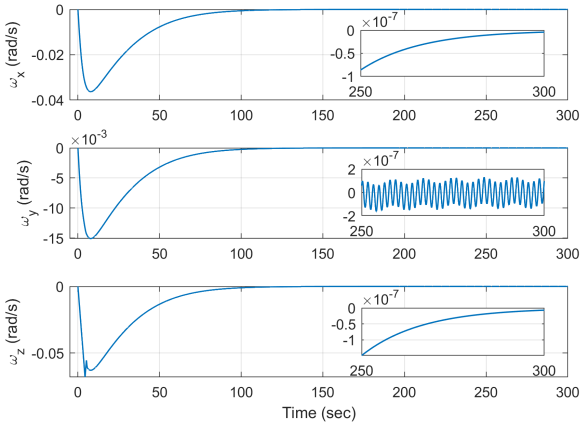

FIGURE 15. Time history of the angular velocity of the controlled system when control torques are saturated at 1600 N•m.

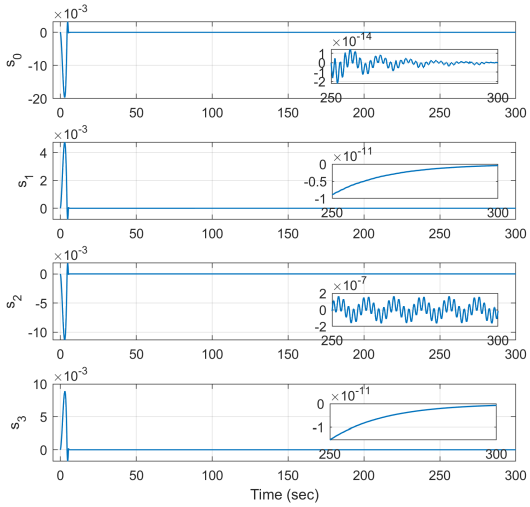

FIGURE 16. Time history of sliding variables when control torques are saturated at 1600 N•m.

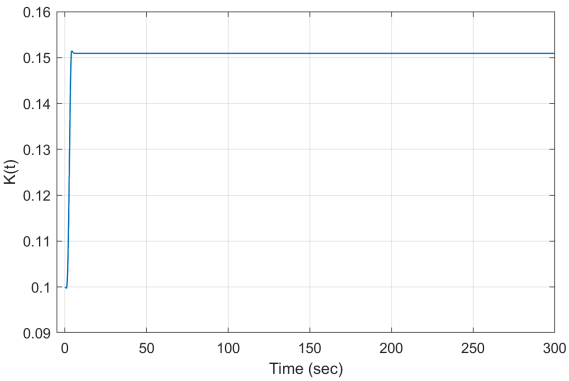

FIGURE 17. Time history of adaptive gain when control torques are saturated at 1600 N•m.

performance for the constrained case. Having similar settling times, the current methodology produces smaller steady-state errors and requires smaller control torques. Table 2 lists the magnitude of the peak control torque and the torque, angular velocity, and quaternion norm at the final time after completing the slew maneuver. It is clearly seen that using

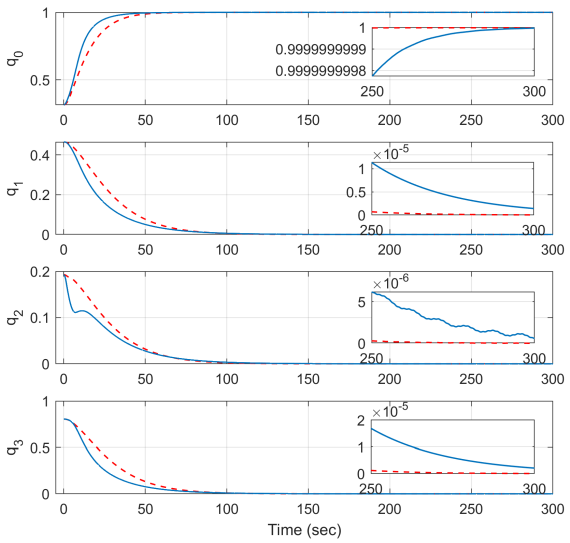

FIGURE 18. Time history of quaternions when the controller proposed in [5] is used (Blue) and when the controller in this paper is used (Red), where control torques are saturated at 1600 N•m for both cases.

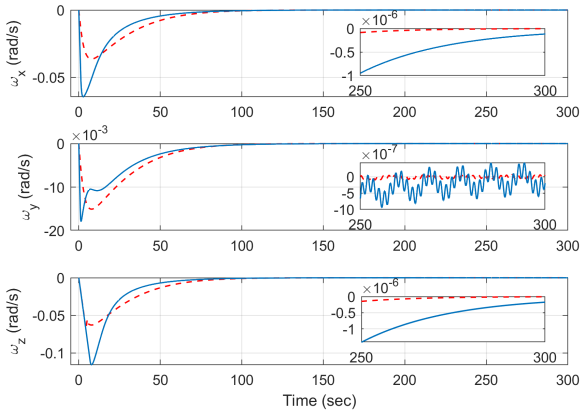

FIGURE 19. Time history of angular velocity when the controller in [5] is used (Blue) and when the controller in this paper is used (Red), where control torques are saturated at 1600 N•m for both cases.

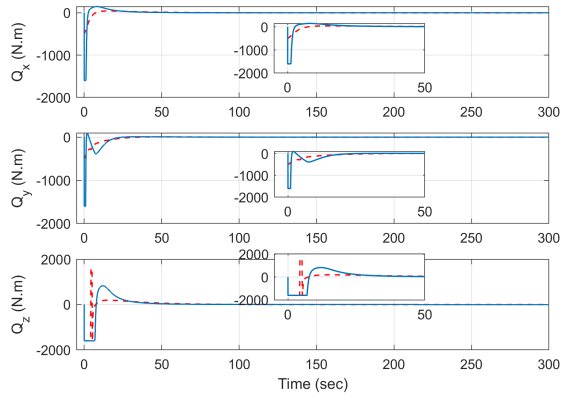

FIGURE 20. Time history of control torques when the controller in [5] is used (Blue) and the controller in this paper is used (Red), where control torques are saturated at 1600 N•m for both cases.

the proposed controller, one can obtain smaller steady-state errors in the angular velocity and quaternion parameters using smaller control torques.

VII. CONCLUSION

This paper proposed two control laws for spacecraft attitude tracking in the presence of model and environmental uncertainties. Once a reference quaternion trajectory is prescribed to satisfy a desired output performance, the first controller assumes a nominal dynamic system with no uncertainties and computes exact optimal control torques to follow the reference trajectory. The solution was obtained with the extended use of the FECM by viewing the attitude tracking requirements as equality constraint and it minimizes the control effort at each instant of time. The second control law assumes an actual, uncertain system to produce smooth control signals that suppress any uncertainty effects. The gain is automatically updated according to the variation of the system uncertainty and any information about the uncertainty bound is not required. As a result, the sliding variables (and the tracking errors) are bounded in finite time within a small ball whose size can be selected by the designer. The proposed control laws have a simple structure and require a small number of control parameters to be tuned, compared to the existing adaptive control approaches. The effect of each control parameter on the control performance was also discussed. A rest-to-rest slew maneuver was numerically simulated to show the robustness and simplicity of the combination of the two control laws proposed in this paper. It was found that the quaternion parameters and angular velocity were successfully controlled to achieve the desired attitude tracking even if the moment of inertia uncertainty and external disturbances were present. The performance of the proposed control methodology was also compared with the existing one, which shows that higher control accuracy and smaller control cost were attained when employing the proposed methodology. The effect of saturation on the control torques was also simulated and discussed. It was shown that the precision attitude tracking in the presence of uncertainties and disturbances could still be achieved in spite of control torque saturation. Also, even with control saturation, the proposed robust control methodology yielded better performance than the existing method. Although it was demonstrated that the norm of the controlled sliding variables was always bounded by ε, it was found in a conservative manner because the simulation results revealed that the actual bound might be much smaller. Hence, finding an exact bound on the norm of the sliding variables is one of our future works. Additionally, the proposed control strategy will be extended to include fault tolerance in its design in the future and its performance will be compared with that of the state-of-the-art achievements such as fault-tolerant adaptive fuzzy control.

REFERENCES

[1] M. Golestani, K. A. Alattas, S. U. Din, F. F. M. El-Sousy, S. Mobayen, and A. Fekih, "A low-complexity PD-like attitude control for spacecraft with full-state constraints," *IEEE Access*, vol. 10, pp. 30707–30715, 2022.

[2] P. Tsiotras, "Further passivity results for the attitude control problem," *IEEE Trans. Autom. Control*, vol. 43, no. 11, pp. 1597–1600, Nov. 1998.

[3] J. Su and K.-Y. Cai, "Globally stabilizing proportional-integral-derivative control laws for rigid-body attitude tracking," *J. Guid., Control, Dyn.*, vol. 34, no. 4, pp. 1260–1264, Jul. 2011.

[4] Y. Su and C. Zheng, "Globally asymptotic stabilization of spacecraft with simple saturated proportional-derivative control," *J. Guid., Control, Dyn.*, vol. 34, no. 6, pp. 1932–1936, Nov. 2011.
[5] K.-S. Kim and Y. Kim, "Robust backstepping control for slew maneuver using nonlinear tracking function," *IEEE Trans. Control Syst. Technol.*, vol. 11, no. 6, pp. 822–829, Nov. 2003.
[6] R. Kristiansen, P. J. Nicklasson, and J. T. Gravdahl, "Satellite attitude control by quaternion-based backstepping," *IEEE Trans. Control Syst. Technol.*, vol. 17, no. 1, pp. 227–232, Jan. 2009.
[7] H. Gao, X. Yang, and P. Shi, "Multi-objective robust H_∞ control of spacecraft rendezvous," *IEEE Trans. Control Syst. Technol.*, vol. 17, no. 4, pp. 794–802, Jul. 2009.
[8] C. Liu, G. Vukovich, K. Shi, and Z. Sun, "Robust fault tolerant non-fragile H_∞ attitude control for spacecraft via stochastically intermediate observer," *Adv. Space Res.*, vol. 62, no. 9, pp. 2631–2648, Nov. 2018.
[9] C. H. Cheng and S. L. Shu, "Application of fuzzy controllers for spacecraft attitude control," *IEEE Trans. Aerosp. Electron. Syst.*, vol. 45, no. 2, pp. 761–765, Apr. 2009.
[10] N. N. Sari, H. Jahanshahi, and M. Fakoor, "Adaptive fuzzy PID control strategy for spacecraft attitude control," *Int. J. Fuzzy Syst.*, vol. 21, no. 3, pp. 769–781, Jan. 2019.
[11] Y. Yu, J. Guo, M. Chadli, and Z. Xiang, "Distributed adaptive fuzzy formation control of uncertain multiple unmanned aerial vehicles with actuator faults and switching topologies," *IEEE Trans. Fuzzy Syst.*, vol. 31, no. 3, pp. 919–929, Mar. 2023, doi: 10.1109/TFUZZ.2022.3193440.
[12] F.-K. Yeh, "Sliding-mode adaptive attitude controller design for spacecrafts with thrusters," *IET Control Theory Appl.*, vol. 4, no. 7, pp. 1254–1264, Jul. 2010.
[13] Z. Ismail, R. Varatharajoo, and Y.-C. Chak, "A fractional-order sliding mode control for nominal and underactuated satellite attitude controls," *Adv. Space Res.*, vol. 66, no. 2, pp. 321–334, Jul. 2020.
[14] V. Utkin, J. Guldner, and J. Shi, *Sliding Mode Control in Electro-Mechanical Systems*. Boca Raton, FL, USA: CRC Press, 2009, pp. 13–15.
[15] J. -J. Slotine and W. Li, *Applied Nonlinear Control*. Englewood Cliffs, NJ, USA: Prentice-Hall, 1991, pp. 276–283.
[16] J. J. Slotine and S. Sastry, "Tracking control of nonlinear systems using sliding surfaces with application to robot manipulator," *Int. J. Control*, vol. 38, no. 2, pp. 465–492, 1983.
[17] H. Cho, G. Kerschen, and T. R. Oliveira, "Adaptive smooth control for nonlinear uncertain systems," *Nonlinear Dyn.*, vol. 99, no. 4, pp. 2819–2833, Mar. 2020.
[18] Y.-J. Huang, T.-C. Kuo, and S.-H. Chang, "Adaptive sliding-mode control for nonlinear systems with uncertain parameters," *IEEE Trans. Syst., Man, Cybern. B, Cybern.*, vol. 38, no. 2, pp. 534–539, Apr. 2008.
[19] S. Mobayen and D. Baleanu, "Stability analysis and controller design for the performance improvement of disturbed nonlinear systems using adaptive global sliding mode control approach," *Nonlinear Dyn.*, vol. 83, no. 3, pp. 1557–1565, Feb. 2016.
[20] F. Plestan, Y. Shtessel, V. Brégeault, and A. Poznyak, "New methodologies for adaptive sliding mode control," *Int. J. Control*, vol. 83, no. 9, pp. 1907–1919, Sep. 2010.
[21] F. Plestan, Y. Shtessel, V. Brégeault, and A. Poznyak, "Sliding mode control with gain adaptation—Application to an electropneumatic actuator," *Control Eng. Pract.*, vol. 21, no. 5, pp. 679–688, May 2013.
[22] H. Cho, F. E. Udwadia, and T. Wanichanon, "Autonomous precision control of satellite formation flight under unknown time-varying model and environmental uncertainties," *J. Astron. Sci.*, vol. 67, no. 4, pp. 1470–1499, Dec. 2020.
[23] H. Cho, "Energy-optimal reconfiguration of satellite formation flying in the presence of uncertainties," *Adv. Space Res.*, vol. 67, no. 5, pp. 1454–1467, Mar. 2021.
[24] S. Mobayen, "Finite-time tracking control of chained-form nonholonomic systems with external disturbances based on recursive terminal sliding mode method," *Nonlinear Dyn.*, vol. 80, nos. 1–2, pp. 669–683, Apr. 2015.
[25] V. Utkin and J. Shi, "Integral sliding mode in systems operating under uncertainty conditions," in *Proc. IEEE CDC*, Kobe, Japan, Dec. 1996, pp. 4591–4596.
[26] J.-H. Lee, "Highly robust position control of BLDDSM using an improved integral variable structure systems," *Automatica*, vol. 42, no. 6, pp. 929–935, Jun. 2006.
[27] S. Mobayen and D. Baleanu, "Linear matrix inequalities design approach for robust stabilization of uncertain nonlinear systems with perturbation based on optimally-tuned global sliding mode control," *J. Vib. control*, vol. 23, no. 8, pp. 1285–1295, May 2017.
[28] F. E. Udwadia and A. D. Schutte, "An alternative derivation of the quaternion equations of motion for rigid-body rotational dynamics," *J. Appl. Mech.*, vol. 77, no. 4, pp. 044505-1–044505-4, Jul. 2010.
[29] F. E. Udwadia and R. E. Kalaba, *Analytical Dynamics: A New Approach*. New York, NY, USA: Cambridge Univ. Press, 1996, pp. 82–84, 101–103, and 109–110.
[30] F. E. Udwadia, T. Wanichanon, and H. Cho, "Methodology for satellite formation-keeping in the presence of system uncertainties," *J. Guid., Control, Dyn.*, vol. 37, no. 5, pp. 1611–1624, Sep. 2014.
[31] T.-T. Lu and S.-H. Shiou, "Inverses of 2 × 2 block matrices," *Comput. Math. Appl.*, vol. 43, nos. 1–2, pp. 119–129, Jan. 2002.
[32] F. E. Udwadia, "Optimal tracking control of nonlinear dynamical systems," *Proc. Roy. Soc. A, Math., Phys. Eng. Sci.*, vol. 464, no. 2097, pp. 2341–2363, Sep. 2008.
[33] C. F. Gauß, "Über rein neues allgemeines grundgsetz der mechanik," *J. Reine Ang. Math.*, vol. 4, pp. 232–235, 1829.
[34] J. Baumgarte, "Stabilization of constraints and integrals of motion in dynamical systems," *Comput. Methods Appl. Mech. Eng.*, vol. 1, no. 1, pp. 1–16, Jun. 1972.
[35] B. Wie, Q. Liu, and F. Bauer, "Classical and robust H_∞ control redesign for the Hubble space telescope," *J. Guid. Control Dyn.*, vol. 16, no. 6, pp. 1069–1077, Nov. 1993.
[36] S. Kumar and S. Chakraborty, "Uncertainty and disturbance-observer based robust attitude control for satellites," *Int. J. Control*, pp. 1–16, Feb. 2022, doi: 10.1080/00207179.2022.2038390.
[37] H. V. Henderson and S. R. Searle, "On deriving the inverse of a sum of matrices," *SIAM Rev.*, vol. 23, no. 1, pp. 53–60, 1981.
[38] Q. Hu, B. Xiao, B. Li, and Y. Zhang, *Fault-Tolerant Attitude Control of Spacecraft*. Amsterdam, The Netherlands: Elsevier, 2021, pp. 231–235.
[39] F. E. Udwadia and P. B. Koganti, "Dynamics and control of a multibody planar pendulum," *Nonlinear Dyn.*, vol. 81, nos. 1–2, pp. 845–866, Mar. 2015.
[40] J. Thienel and R. Sanner, "Hubble space telescope angular velocity estimation during the robotic servicing mission," *J. Guid. Control Dyn.*, vol. 30, no. 1, pp. 29–34, Jan. 2007.

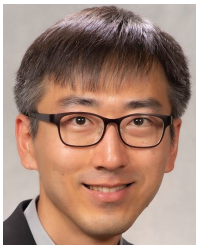

HANCHEOL CHO (Member, IEEE) received the B.S. and M.S. degrees in astronomy from Yonsei University, Seoul, South Korea, in 2006 and 2008, respectively, and the Ph.D. degree in aerospace engineering from the University of Southern California, Los Angeles, CA, USA, in 2012.

From 2013 to 2015, he was a Senior Research Engineer with Samsung Techwin Company Ltd. He was a Marie-Curie COFUND Postdoctoral Fellow with the University of Liege, Liege, Belgium, and a Postdoctoral Appointee with the Sandia National Laboratories, Albuquerque, NM, USA. From 2019 to 2021, he was an Assistant Professor with the Mechanical Engineering Department, Bradley University, Peoria, IL, USA. Since 2021, he has been an Assistant Professor with the Aerospace Engineering Department, Embry-Riddle Aeronautical University, Daytona Beach, FL, USA. His research interests include robust adaptive controls, astrodynamics, optimization, and robotics. He is an Associate Editor of the *Journal of Control, Automation and Electrical Systems* (Springer).